Inorg. Chem. **2004**, *43*, 5908–5918

New Route to the Mixed Valence Semiquinone-Catecholate Based Mononuclear Fe^{III} and Catecholate Based Dinuclear Mn^{III} Complexes: First Experimental Evidence of Valence Tautomerism in an Iron Complex

Nizamuddin Shaikh,[†,‡] Sanchita Goswami,[†] Anangamohan Panja,[†] Xin-Yi Wang,[§] Song Gao,[§] Ray J. Butcher,[||] and Pradyot Banerjee*[,†]

Department of Inorganic Chemistry, Indian Association for the Cultivation of Science, Kolkata 700 032, India, College of Chemistry and Molecular Engineering, State Key Laboratory of Rare Earth Materials Chemistry and Applications, Peking University, Beijing, P. R. China, and Department of Chemistry, Howard University, 2400 Sixth Street, NW, Washington, D.C. 20059

Received March 31, 2004

The semiquinone-catecholate based mixed valence complex, $[Fe^{III}(bispicen)(Cl_4Cat)(Cl_4SQ)]\cdot DMF$ (**1**), and catecholate based $(H_2bispictn)[Mn_2^{III}(Cl_4Cat)_4(DMF)_2]$ (**2**) (bispicen = *N*,*N*′-bis(2-pyridylmethyl)-1,2-ethanediamine, bispictn = *N*,*N*′-bis(2-pyridylmethyl)-1,3-propanediamine, Cl_4Cat = tetrachlorocatecholate dianion, and Cl_4SQ = tetrachlorosemiquinone radical anion) were synthesized directly utilizing a facile route. Both the complexes have been characterized by single crystal X-ray diffraction study. The electronic structures have been elucidated by UV–vis–NIR absorption spectroscopy, cyclic voltammetry, EPR, and magnetic properties. The structural as well as spectroscopic features support the mixed valence tetrachlorosemiquinone-tetrachlorocatecholate charge distribution in **1**. The ligand based mixed valence state was further confirmed by the presence of an intervalence charge transfer (IVCT) band in the 1900 nm region both in solution and in the solid. The intramolecular electron transfer, a phenomenon known as valence tautomerism (VT), has been followed by electronic absorption spectroscopy. For **1**, the isomeric form $[Fe^{III}(bispicen)(Cl_4Cat)(Cl_4SQ)]$ is favored at low temperature, while at an elevated temperature, the $[Fe^{II}(bispicen)(Cl_4SQ)_2]$ redox isomer dominates. Infrared as well as UV–vis–NIR spectral characterization for **2** suggest that the $Mn^{III}(Cat)_2^-$ moiety is admixed with its mixed valence semiquinone-catecholate isomer $Mn^{II}(SQ)(Cat)^-$, and the electronic absorption spectrum is dominated by the mixed charged species. The origin of the intervalence charge transfer band in the 1900 nm range is associated with the mixed valence form, $Mn^{II}(Cl_4Cat)(Cl_4SQ)^-$. The observation of VT in complex **1** is the first example where a mixed valence semiquinone-catecholate iron(III) complex undergoes intramolecular electron transfer similar to manganese and cobalt complexes.

Introduction

Transition metal coordination chemistry of ligands derived from catecholate and *o*-benzoquinone has been the subject of intensive research for the last few decades,[1,2] particularly for their rich redox properties and potential for forming compounds that may exist in a number of electronic states owing to the combined electrochemical activity of the metal ion and one or more quinone ligands.[3] The degree of freedom of the electronic states is due to the redox forms of catecholate (cat^{2-}), *o*-semiquinonate ($SQ^{\bullet -}$), and *o*-benzoquinone (BQ). Recent studies show that the delicate balance of the distribution of the charge and the spin over the whole molecule results in "valence tautomerism" (VT).[4,5] VT has

* To whom correspondence should be addressed. E-mail: icpb@mahendra.iacs.res.in.
† Indian Association for the Cultivation of Science.
‡ Present address: Department of Biochemistry, Center for Chemistry and Chemical Engineering, University of Lund, Sweden.
§ Peking University.
|| Howard University.

(1) Pierpont, C. G.; Buchanan, R. M. *Coord. Chem. Rev.* **1981**, *38*, 45.
(2) Pierpont, C. G.; Lange, C. W. *Prog. Inorg. Chem.* **1994**, *41*, 331.
(3) Röhrscheid, F.; Balch, A. L.; Holm, R. H. *Inorg. Chem.* **1966**, *5*, 1542.
(4) Pierpont, C. G. *Coord. Chem. Rev.* **2001**, *216*−*217*, 99.

10.1021/ic049579i CCC: $27.50
Published on Web 08/25/2004

been observed for the manganese and cobalt complexes, and their attractiveness is due to the fact that the physical behaviors of these complexes are similar to those of the metal complexes exhibiting spin-crossover whose reversible transformations can be utilized for creating addressable memories.[6,7]

In view of this, a series of mixed-valence semiquinone-catecholate transition metal complexes have been prepared and characterized by single crystal X-ray diffraction study.[8−12] The synthetic procedures employed for the preparation of mixed valence Cr, Mn, Co, and other transition metal complexes involve the reaction of substituted *o*-benzoquinone and the neutral metal carbonyl in which the metals are in zero oxidation states, and consequent reduction of the former leads to the formation of the desired products under an inert atmosphere. A number of $Fe^{III}(SQ)_3$ complexes have been characterized with the four common semiquinone ligands Cl_4-SQ, PhenSQ, 3,5-DBSQ, and 3,6-DBSQ in which metal ion is found to be high-spin iron(III) at all temperatures.[8] Mixed valence semiquinone-catecholate iron complexes (e.g., [Fe(3,5-DBSQ)(3,5-DBCat)(bpy)], [Fe(DBSQ)(DBCat)(phen)], [Fe(phenSQ)(phenCat)(phen)]·THF, etc.) have been subsequently prepared by treating the corresponding $Fe(SQ)_3$ complexes with suitable reducing agents.[13] Utmost care has also been exercised to prevent the decomposition of the semiquinone radical chelated complexes.[9−18] A majority of them have been characterized by single crystal X-ray diffraction, and their spectroscopic studies and magnetic measurements were done in the solid state and in solution.[9−22] Among these, semiquinone and catecholate chelated cobalt and manganese complexes have gathered special attention due to the temperature dependent "VT" involving intramolecular electron transfer from the ligand to metal or vice versa.[4,5] Equilibria between Co^{III} and Co^{II} redox isomers (eq 1) have been observed by monitoring the magnetism and electronic spectral changes which suggest the shift from low-spin Co^{III} to high-spin Co^{II}.[4,23−24]

$$Co^{III}(N-N)(SQ)(Cat) \rightleftharpoons Co^{II}(N-N)(SQ)_2 \qquad (1)$$

For manganese, three redox isomers are possible, and the equilibria occur in two steps (eqs 2 and 3).[9−11,25]

$$Mn^{IV}(N-N)(Cat)_2 \rightleftharpoons Mn^{III}(N-N)(SQ)(Cat) \qquad (2)$$

$$Mn^{III}(N-N)(SQ)(Cat) \rightleftharpoons Mn^{II}(N-N)(SQ)_2 \qquad (3)$$

A dramatic thermochromic effect in solution[17] was noted for the mononuclear $Mn(py)_2(3,5\text{-DBCat})_2$. Similar changes in the optical spectrum were also observed for the tetranuclear complex, $[Mn^{II}(3,5\text{-DBSQ})_2]_4$, and the following equilibrium (eq 4) is operative in this instance.

$$Mn^{IV}(py)_2(3,5\text{-DBCat})_2 \rightleftharpoons Mn^{II}(py)_2(3,5\text{-DBSQ})_2 \qquad (4)$$

As with Co and Mn complexes, it is important to mention that the observations of VT are not restricted to the $Mn(N-N)(DBSQ)_2$ series.[26−29] Dei et al. have isolated and characterized both the ($[Mn^{III}(CTH)(3,5\text{-DBCat})]^+$) and ($[Mn^{II}(CTH)(3,5\text{-DBSQ})]^+$) isomers using a tetradentate ligand.[26] Thermal equilibria were observed for these compounds in the solid state as well as in solution. Several other dioxolene ligands have also been successfully used to obtain transition metal complexes with interesting properties.[27−29]

Iron, which lies between Mn and Co in the first transition series, is also expected to show redox isomerism of the type

$$[Fe^{III}(N-N)(SQ)(Cat)] \rightleftharpoons [Fe^{II}(N-N)(SQ)_2] \qquad (5)$$

But, so far, no behavior in the solid state or in solution has yet been noted to justify that the complexes undergo tautomeric equlibria of the type shown here.

Apart from the materials interest of the iron-semiquinone complexes, a number of enzymes have been implicated to involve iron−semiquinone intermediates.[30] The intradiol catechol dioxygenases which catalyze the cleavage of the carbon−carbon bond between the two hydroxyl groups, for example, contains non-heme iron(III) cofactor, and the catalytic cycle has been proposed to involve iron−semiquinone as an intermediate.[30] The study of the transition

(5) Pierpont, C. G. *Coord. Chem. Rev.* **2001**, *219−221*, 415.
(6) (a) Gütlich, P.; Hauser, A.; Spiering, H. *Angew. Chem.* **1994**, *106*, 2109. (b) Gütlich, P.; Hauser, A.; Spiering, H. *Angew. Chem., Int. Ed. Engl.* **1994**, *33*, 2024.
(7) Kahn, O.; Jay-Martinez, C. *Science* **1998**, *279*, 44.
(8) Cohn, M. J.; Xie, C.-L.; Tuchagues, J.-P. M.; Pierpont, C. G.; Hendrickson, D. N. *Inorg. Chem.* **1992**, *31*, 5028.
(9) Attia, A. S.; Pierpont, C. G. *Inorg. Chem.* **1995**, *34*, 1172.
(10) Attia, A. S.; Pierpont, C. G. *Inorg. Chem.* **1998**, *37*, 3051.
(11) Attia, A. S.; Pierpont, C. G. *Inorg. Chem.* **1997**, *36*, 6184.
(12) Larsen, S. K.; Pierpont, C. G.; DeMunno, G.; Dolcetti, G. *Inorg. Chem.* **1986**, *25*, 4828.
(13) Lynch, M. W.; Valentine, M.; Hendrickson, D. N. *J. Am. Chem. Soc.* **1982**, *102*, 6982.
(14) Chang, H.-C.; Ishii, T.; Kondo, M.; Kitagawa, S. *J. Chem. Soc., Dalton Trans.* **1999**, 2467.
(15) Chang, H.-C.; Kitagawa, S. *Angew. Chem., Int. Ed.* **2002**, *41*, 130.
(16) (a) Chang, H.-C.; Kitagawa, S. *Angew. Chem., Int. Ed.* **2002**, *41*, 4444. (b) Cador, O.; Chabre, F.; Dei, A.; Sangregorio, C.; Van Slageren, J.; Vaz, M. G. F. *Inorg. Chem.* **2003**, *42*, 6432.
(17) Lynch, M. W.; Hendrickson, D. N.; Fitzgerald, B. J.; Pierpont, C. G. *J. Am. Chem. Soc.* **1984**, *106*, 2041.
(18) Buchanan, R. M.; Pierpont, C. G. *J. Am. Chem. Soc.* **1980**, *102*, 4951.
(19) Attia, A. S.; Bhattacharya, S.; Pierpont, C. G. *Inorg. Chem.* **1995**, *34*, 4427.
(20) Jung, O.-S.; Jo, D. H.; Lee, Y. A.; Conklin, B. J.; Pierpont, C. G. *Inorg. Chem.* **1997**, *36*, 19.
(21) Jung, O.-S.; Pierpont, C. G. *Inorg. Chem.* **1994**, *33*, 2227.
(22) (a) Zirong, D.; Bhattacharya, S.; McCusker, J. K.; Hagen, P. M.; Hendrickson, D. N.; Pierpont, C. G. *Inorg. Chem.* **1992**, *31*, 870. (b) Velusamy, M.; Palaniandavar, M.; Gopalan, R. S.; Kulkarni, G. U. *Inorg. Chem.* **2003**, *42*, 8283. (c) Panja, A.; Shaikh, N.; Gupta, S.; Butcher, R. J.; Banerjee, P. *Eur. J. Inorg. Chem.* **2003**, 1540.
(23) Jung, O.-S.; Pierpont, C. G. *J. Am. Chem. Soc.* **1994**, *116*, 2229.
(24) Adams, D. M.; Noodleman, L.; Hendrickson, D. N. *Inorg. Chem.* **1997**, *36*, 3966.
(25) Attia, A. S.; Jung, O.-S.; Pierpont, C. G. *Inorg. Chim. Acta* **1994**, *226*, 91.
(26) Caneschi, A.; Dei, A. *Angew. Chem., Int. Ed.* **1998**, *37*, 3005.
(27) Caneschi, A.; Dei, A.; Mussari, C. P.; Shultz, D. A.; Sorace, L.; Vostrikova, K. E. *Inorg. Chem.* **2002**, *41*, 1086.
(28) Caneschi, A.; Dei, A.; Gatteschi, D.; Tangoulis, V. *Inorg. Chem.* **2002**, *41*, 3508.
(29) Bodnar, S. H.; Caneschi, A.; Dei, A.; Shultz, D. A.; Sorace, L. *Chem. Commun.* **2001**, 2150.
(30) (a) Que, L., Jr.; Ho, R. Y. N. *Chem. Rev.* **1996**, *96*, 2607. (b) Bugg, T. D. H.; Winfield, C. J. *Nat. Prod. Rep.* **1998**, 15, 513. (c) Funabiki, T.; *Catalysis by metal complexes*; Kluwer Academic Publishers: Dordrecht, 1997; p 19. (d) Funabiki, T.; Mizoguchi, A.; Sugimoto, T.; Tada, S.; Tsuji, M.; Sakamoto, H.; Yoshida, S. *J. Am. Chem. Soc.* **1986**, *108*, 2921.

Chart 1

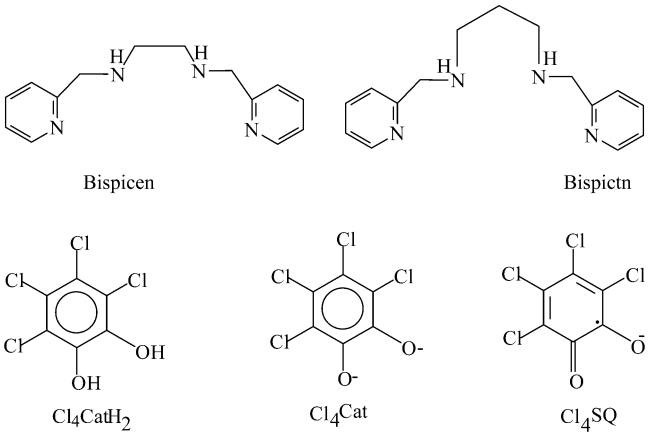

metal−semiquinone complexes is, therefore, worth studying from the materials as well as bioinorganic points of view.

Herein, we report the syntheses, structures, and spectroscopic and magnetic properties of the mononuclear mixed valence tetrachlorosemiquinone-tetrachlorocatecholate iron(III) and tetrachlorocatecholate chelated hydrogen bonded dinuclear manganese(III) complexes prepared directly by a facile route using tetradentate N-donor ligands, namely bispicen (bispicen = *N*,*N*′-bis(2-pyridylmethyl)-1,2-ethanediamine) and bispictn [bispictn = *N*,*N*′-bis(2-pyridylmethyl)-1,3-propanediamine] (Chart 1). Experimental evidence has been gathered for the VT phenomenon in the iron complex for the first time in solution as well as in the solid state.

Experimental Section

Materials. All materials used were of reagent grade. Pyridine-2-carboxaldehyde and tetrachlorocatechol monohydrate ($Cl_4CatH_2 \cdot H_2O$) were purchased from Aldrich. Both 1,2-diaminoethane and 1,3-diaminopropane were distilled prior to the reaction. The ligands (bispicen and bispictn) as well as the complexes [Fe^{III}(bispicen)Cl_2]Cl and [Mn^{II}(bispictn)Cl_2] were prepared following the literature procedures.[31] The reagents and solvents were used without further purification. Distilled water was used throughout.

Complex Syntheses. [Fe^{III}(bispicen)(Cl_4Cat)(Cl_4SQ)]·DMF (1). To an aqueous solution (10 cm^3) of [Fe(bispicen)Cl_2]Cl (0.40 g, 1 mmol) was added a DMF solution (30 cm^3) of tetrachlorocatechol monohydrate (0.52 g, 2 mmol). The mixture was stirred in air for 10 min whereby a deep blue solution was formed. It was filtered and kept in air. Deep blue crystals of complex **1** were obtained after 4−5 days and were then filtered and washed first by the mother liquor followed by diethyl ether and dried in air. (Yield = 70% based on Fe.)

Anal. Calcd for $C_{26}H_{18}N_4O_4Cl_8Fe \cdot 0.5DMF$: C, 39.93; H, 2.60; N, 7.62. Found: C, 40.14; H, 2.71; N, 7.63%.

(H_2bispictn)[Mn_2^{III}(Cl_4Cat)$_4$(DMF)$_2$] (2). To an aqueous solution (10 cm^3) of [Mn(bispictn)Cl_2] (0.38 g, 1 mmol) was added a DMF solution (20 cm^3) of tetrachlorocatechol monohydrate (0.26 g, 1 mmol), and the reaction mixture was stirred in air. A clear green solution was thereby formed which was filtered to remove any suspended materials. The solution was kept in air. Needle shaped green crystals of **2** were formed within 12 h. They were filtered and washed first by the mother liquor followed by diethyl ether with the addition of a little DMF and dried in air. (Yield = 75% based on Mn.)

Anal. Calcd for $C_{45}H_{35}N_6O_{10}Cl_{16}Mn_2$: C, 36.12; H, 2.32; N, 5.61. Found: C, 36.13; H, 2.24; N, 5.71%.

Table 1. Crystallographic Data Collection and Refinement Data for **1** and **2**

	1	**2**
formula	$C_{27.5}H_{21.5}Cl_8FeN_{4.5}O_{4.5}$	$C_{45}H_{35}Cl_{16}Mn_2N_6O_{10}$
fw	826.44	1496.87
cryst syst	monoclinic	monoclinic
space group	*P*21/*c* (No. 14)	*C*2/*c* (No. 15)
a, Å	9.33(2)	21.061(6)
b, Å	28.72(8)	15.918(5)
c, Å	10.81(2)	18.498(3)
β, deg	92.19(8)	114.986(6)
V, Å^3	2895(11)	5621(3)
Z	4	4
ρ, g/cm^3	1.896	1.769
μ(Mo Kα), mm^{-1}	1.310	1.272
T, K	93	93
λ, Å (Mo Kα)	0.71073	0.71073
$\theta_{min-max}$, deg	2.0−26.4	1.8−29.3
total data	19443	24648,
unique data (R_{int})	5823 (0.086)	7152 (0.042)
observed data [$I > 2.0\sigma(I)$]	4910	5450
R, wR2	0.0777, 0.2139	0.0348, 0.0779

Physical Measurements. Microanalysis (CHN) was performed on a Perkin-Elmer 240C elemental analyzer. The EPR spectra were obtained on a Varian model 109 E-line X-band spectrometer equipped with a low-temperature quartz Dewar for low-temperature measurements. FT-IR spectra were obtained on a Nicolet MAGNA-IR 750 spectrometer with samples prepared as KBr pellets. Cyclic voltammetry (scan rate of 0.05 V s^{-1}) was performed at a platinum electrode using an EG&G PARC electrochemical analysis system (model 250/5/0) in acetonitrile under dry nitrogen atmosphere in conventional three-electrode configurations. UV−vis−NIR spectroscopic measurements were carried out on a JASCO V-750 spectrophotometer equipped with thermostated cell compartments. Variable temperature magnetic susceptibility and field dependence of magnetization measurements were performed on an Oxford Maglab 2000 system.

Crystallographic Data Collection and Refinement of Structures. Single crystals of both **1** and **2** were grown from a DMF−water mixture. Each crystal was then mounted on an automatic Bruker P4 diffractometer equipped with a graphite monochromated Mo Kα radiation (λ = 0.71073 Å). Unit cell dimensions and intensity data were measured at 93 K both for **1** and **2**. The structures were solved by direct methods and refined by full-matrix least-squares based on F^2 with anisotropic thermal parameters for non-hydrogen atoms using Bruker SHELXTL (data reduction), SHELXS[32] (structure solution), and SHELXL[33] (structure refinement). The hydrogen atoms were included in structure factor calculations in their idealized position. Information concerning crystallographic data collection and refinement of the structures is compiled in Table 1.

Results and Discussion

Synthesis. The tetradentate bispicen and bispictn ligands (bispicen = *N*,*N*′-bis(2-pyridylmethyl)-1,2-ethanediamine and

(31) Toftlaund, H.; Pedersen, E.; Yde-Andersen, S. *Acta Chem. Scand., Ser. A* **1984**, *38*, 693.

(32) Sheldrick, G. M. *SHELXS 97*, *Acta Crystallogr., Sect. A* **1990**, *46*, 467.

(33) Sheldrick, G. M. *SHELXL 97, Program for Crystal Structure Refinement*; University of Göttingen: Göttingen, Germany, 1997.

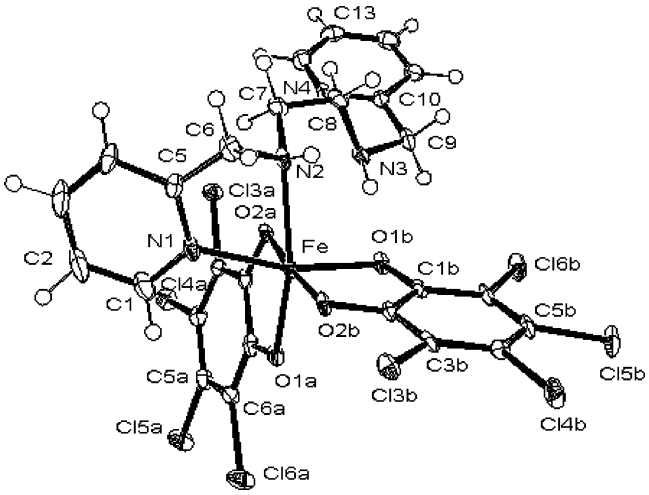

Figure 1. Molecular view of [Fe^{III}(bispicen)(Cl_4SQ)(Cl_4Cat)]·DMF (**1**) showing atom labeling schemes.

bispictn = *N*,*N*′-bis(2-pyridylmethyl)-1,3-propanediamine) used in the present study are known to form transition metal complexes with two labile chloride ions in *cis*-position.[31] We reasoned that this disposition of chloride ions might give rise to two vacant coordination sites in solution, and thereby, chelation of the 1,2-dihydroxybenzenes would generate an intermediate complex which in the presence of aerial O_2 might lead to the formation of the semiquinone chelated products. The complexes prepared by the reaction of alkyl substituted catechols (e.g., 4-*tert*-butylcatechol and 3,5-di-*tert*-butylcatechol) were found to be extremely air sensitive leading to the formation of intractable products presumably due to the oxygenation of the substituted catechols.[34,35] The reaction of *cis*-[Fe^{III}(bispicen)Cl_2]Cl and tetrachlorocatechol (Cl_4CatH_2) in DMF−water mixture, however, produced mixed valence tetrachlorosemiquinone-tetrachlorocatecholate iron(III) complex of molecular formula [Fe^{III}(Cl_4Cat)(Cl_4SQ)(bispicen)]·DMF as dark blue crystals. On the other hand, the reaction of *cis*-[Mn^{II}(bispictn)Cl_2] and tetrachlorocatechol produced green crystals of a manganese(III) complex which corresponds to the molecular formula (H_2bispictn)[Mn_2^{III}(Cl_4Cat)$_4$(DMF)$_2$]. The novelty in the synthetic procedure applied to obtain the present complexes lies in the fact that, unlike that reported for the other mixed-valence semiquinone-catecholate and/or catecholate chelated transition metal complexes, it does not require any inert atmosphere. Moreover, no externally added bases such as NaOH or triethylamine are required for the reaction to occur.[9−13]

Crystal Structure of [Fe^{III}(bispicen)(Cl_4Cat)(Cl_4SQ)]·DMF (1). A dark blue crystal of complex [Fe^{III}(bispicen)(Cl_4Cat)(Cl_4SQ)]·DMF (**1**) was obtained as DMF solvates. A drawing of the complex molecule is shown in Figure 1, and important bond distances and angles appear in Table 2. The geometry of the central Fe^{III} ion is roughly octahedral. The in-plane positions are occupied by $N1_{pyridine}$, $N2_{amine}$, O1A, and O1B around the Fe^{III}, and the axial positions are occupied by O2A and O2B having O2A−Fe−O2B bond angle 174.91°. The remaining two N (one pyridine and one amine) atoms of the bispicen ligand are uncoordinated. The free amine proton is involved in strong H-bonding interaction with the catecholate oxygen atom (N3−H···O2A = 2.645(10) Å) stabilizing the ligand. The Fe−O1A and Fe−O2A bond distances are 1.797(6) and 2.033(7) Å whereas Fe−O1B and Fe−O2B are 1.910(7) and 1.960(7) Å. The Fe−$N1_{pyridine}$ and Fe−$N2_{amine}$ bond distances are 2.084(8) and 2.186(8) Å, respectively. The C−O lengths for the chelated ligand containing O1A and O2A are 1.235(8) and 1.139(7) Å, and those for the ligand containing O1B and O2B are 1.329(8) and 1.267(7) Å. The semiquinone ligands generally have shorter C−O bond lengths (1.28 Å) than the fully reduced catecholate ligand (1.34−1.35 Å).[22a]

Table 2. Selected Bond Distances (Å) and Angles (deg) for **1**

Fe−O1A	1.797(6)	Fe−O2A	2.033(7)
Fe−O1B	1.910(7)	Fe−O2B	1.960(7)
Fe −N1	2.084(8)	Fe−N2	2.186(8)
C1A−O1A	1.235(8)	C2A−O2A	1.139(7)
C1B−O1B	1.329(8)	C2B−O2B	1.267(7)
C1A−C2A	1.592(10)	C1B−C2B	1.434(8)
O1A−Fe−O1B	99.34(19)	O1A−Fe−O2A	98.66(19)
O1A−Fe−O2B	82.77(19)	O1A−Fe−N1	95.2(2)
O1A−Fe−N2	166.0(2)	O1B−Fe−O2A	89.12(19)
O1B−Fe−O2B	85.78(18)	O1B−Fe−N1	165.4(2)
O2A−Fe−O2B	174.86(17)	O2A−Fe−N1	90.2(2)
O2A−Fe−N2	72.72(19)	O2B−Fe−N1	94.6(2)
O2B−Fe−N2	106.81(19)	N1−Fe−N2	74.3(2).

The structurally characterized complex [Fe^{III}(3,6-DBSQ)(3,6-DBCAT)(bpy)] has an average C−O bond length of 1.308(4) Å whereas it is 1.311 Å[19] for [Co(bpy)(3,6-DBSQ)(3,6-DBCAT)]. The anionic complex, Fe(bpy)($Cl_4Cat)_2^-$, has the average C−O bond distances of 1.327 and 1.312 Å for the two catecholate ligands.[22a] An average value of 1.310(5) Å of C−O bond lengths for *trans*-[Cr^{III}(Cl_4SQ)(Cl_4Cat)($CH_3CN)_2$] has, however, been reported recently.[16] The average C−O bond lengths for **1** are significantly shorter compared to those of the previously reported mixed valence semiquinone-catecholato iron(III) complexes.[19] The differences of the C−O bond lengths, however, imply a localized mixed-valence state for the two quinonate ligands. A similar conclusion can be drawn from the Fe−O bond distances. The average Fe−O bond distances [Fe−O1A = 1.797(6) Å, Fe−O2A = 2.033(7) Å, Fe−O1B = 1.910(7) Å, and Fe−O2B = 1.960(7) Å] are shorter than those observed in [Fe(bpy)($Cl_4Cat)_2]^-$ where the values for the two chelated catecholate ligands are 1.983 and 1.992 Å.[22a] The average Fe−O bond length of 1.925 Å is, however, close to an average Cr−O bond length of 1.932(3) Å in [Cr^{III}(Cl_4SQ)(Cl_4Cat)(L)] complexes.[16] In summary, the structural features of **1** are close to the trivalent state of iron and the presence of mixed-valence forms of the dioxolene ligands. Further confirmation is apparent from the spectroscopic studies.

Crystal Structure of (H_2bispictn)[Mn_2^{III}(Cl_4Cat)$_4$(DMF)$_2$] (2). Complex **2** could be viewed as composed of a dicationic bispictn ligand (H_2bispictn) and the anionic [Mn_2^{III}(Cl_4Cat)$_4$(DMF)$_2]^{2-}$ moiety. The dicationic form of the ligand is due to the protonation of both of the amine nitrogen and the protonated hydrogen atoms participating in a hydrogen

(34) Funabiki, T.; Mizoguchi, A.; Sugimoto, T.; Tada, S.; Tsuji, M.; Sakamoto, H.; Yoshida, S. *J. Am. Chem. Soc.* **1986**, *108*, 2921.
(35) Shaikh, N.; Panja, A.; Ali, M.; Banerjee, P. *Transition Met. Chem.* **2003**, *28*, 881.

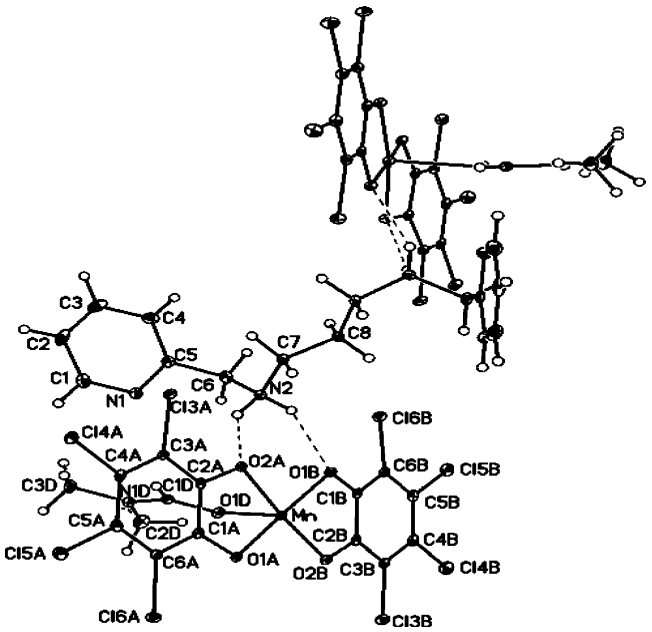

Figure 2. Molecular structure of dimeric $(H_2bispictn)[Mn_2^{III}(Cl_4Cat)_4(DMF)_2]$ (**2**) with atom labeling schemes.

Table 3. Selected Bond Distances (Å) and Angles (deg) and Hydrogen Bonds for **2**

Mn−O1A	1.8968(16)	Mn−O1B	1.9220(17)
Mn−O1D	2.1940(19)	Mn−O2A	1.8960(15)
Mn−O2B	1.8939(15)	Mn−O1B_a	2.8354(19)
O1A−C1A	1.345(2)	O1B−C1B	1.354(3)
O2A−C2A	1.355(3)	O2B−C2B	1.343(3)
C1A−C2A	1.409(3)	C1B−C2B	1.413(3)
O1A−Mn−O1B	171.50(7)	O1A−Mn−O1D	96.34(7)
O1A−Mn−O2A	86.48(6)	O1A−Mn−O2B	96.70(6)
O1A−Mn−O1B_a	87.37(6)	O1B−Mn−O1D	91.64(7)
O1B−Mn−O2A	90.45(6)	O1B−Mn−O2B	85.89(6)
O1D−Mn−O2A	91.29(6)	O1D−Mn−O2B	92.00(6)
O2A−Mn−O2B	175.15(8)	O1B_a−Mn−O2A	83.81(6)
O1B_a−Mn−O2B	92.66(6)		
N2−H2A···O2A	2.779(2)	N2−H2A···N1	2.862(3)
N2−H2C···O1B	2.822(2)		

bonding interaction with the O atoms of the chelated ligands. A molecular view of complex **2** with atom-labeling schemes is shown in Figure 2. Selected bond distances and angles are given in Table 3. The geometry of each manganese center is square pyramidal. Oxygen atoms from two dioxolene ligands occupy the in-plane positions. Bond lengths from the manganese to oxygen donor atoms for Mn−O1A and Mn−O2A are 1.8968(16) and 1.8960(15) Å, whereas those of the Mn−O1B and Mn−O2B are 1.922(17) and 1.8939(15) Å, respectively. These are similar to the Mn−O lengths observed for catecholato manganese(III) complexes.[9−11] The semiquinone ligands generally have shorter C−O bond lengths (1.28 Å) than the fully reduced catecholate ligand (1.34−1.35 Å). The average C−O bond distance (1.349(3) Å) of the chelated dioxolene ligands which are sensitive to charge distribution is fully consistent with Mn^{III}−Cat charge distribution.[9−11] The C−C bond lengths of 1.409(4) and 1.413(3) Å bearing catecholate −OH also support Mn^{III}−Cat formulation. Mn−O and C−O bond distances observed for **2** also compare well with the recently reported polymeric manganese(II,III) complex chelated by the tetrachlorocatecholate ligands.[36a] The DMF solvent molecule occupying the apical position of the square pyramidal geometry around the metal center with Mn−O bond length of 2.1940(19) Å is axially elongated and expected for a high-spin Mn^{III} having d^4 electronic configuration. A crystallographic inversion center generates a second monomeric unit so that the planar catecholate ligands of the adjacent unit lie in the dimeric face to face orientation as in Figure 3. The cationic bispictn ligand is held by hydrogen bonding interaction involving the N−H proton from the ligand and the coordinating O atom of the chelated catecholate oxygen atoms [N2−H2A···O2A = 2.779(2) Å and N2−H2C···O1B = 2.822(2) Å]. The hydrogen bond distances are significantly short, and therefore, the interaction is strong enough to render the molecule a dinuclear nature in the solid state. Catecholate oxygen O1B of the adjacent Mn^{III} unit located at the sixth coordination site of Mn atom with a Mn−O1B distance of 2.8354(19) Å also helps in the stabilization of the dimeric unit (Figure 3). The Mn−Mn separation is 3.5766(12) Å in the present complex. This structure is essentially identical to that reported for $[Mn^{III}(Br_4Cat)_2(OPPh_3)]^-$ by Larsen et al.[12] The bispictn ligand additionally participates in the stabilization of the crystal lattice unlike the former.

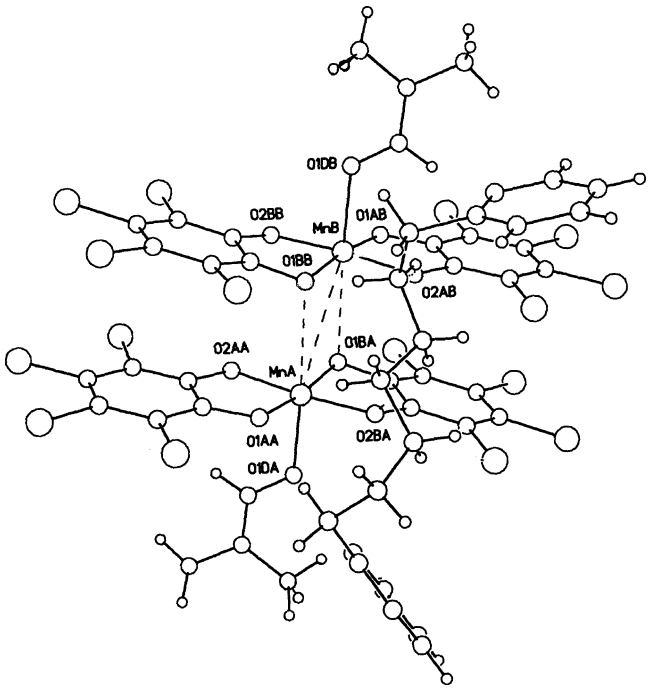

Figure 3. Molecular view showing nonbonding interaction between the manganese centers and dimeric face-to-face orientation of the planer catecholate ligands in complex **2**.

FT-IR Spectroscopy. Infrared spectra of the metal−quinone complexes serve as an important tool to distinguish between the catecholate and semiquinonate ligands. The IR spectra of both the complexes were taken as KBr pellets. The semiquinone ligands while chelated to the metal usually show strong absorption bands in the range 1420−1460 cm^{-1}. The spectrum of complex **1** is depicted by a strong absorption

(36) (a) Shaikh, N.; Panja, A.; Goswami, S.; Banerjee, P.; Vojtisek, P.; Zhang, Y.-Z.; Su, G.; Gao, S. *Inorg. Chem.* **2004**, *43*, 849. (b) Shaikh, N.; Panja, A.; Gao, S.; Banerjee, P. Manuscript in preparation.

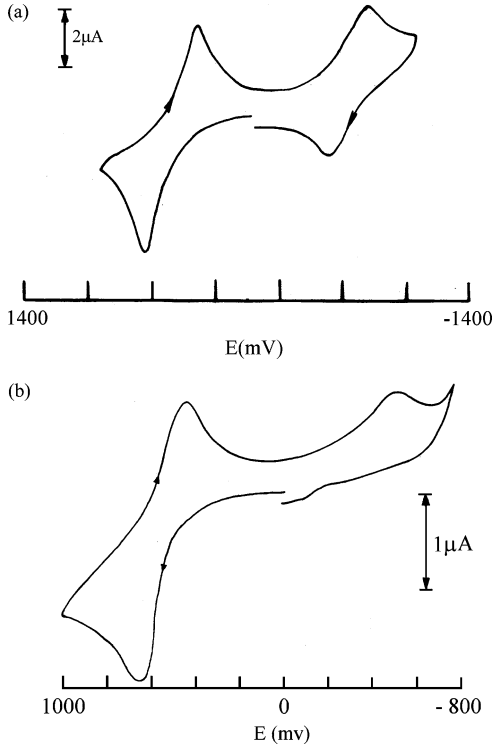

Figure 4. Cyclic voltammogram (scan rate 50 mV s^{-1}) of complex **1** (a) and **2** (b) in acetonitrile at a platinum electrode with ferrocene as an internal standard and TEAP as supporting electrolyte.

band at 1440 cm^{-1} and a relatively less intense band at 1247 cm^{-1} whereas the corresponding bands for **2** are observed at 1421 and 1250 cm^{-1}. These are characteristic for the ligand based mixed valence semiquinone-catecholate transition metal complexes.[12−17] The bands at 1100 and 1480 cm^{-1} are generally observed for catecholate based transition metal complexes which are present for **2**, but not for **1**. The strong absorption band at 1421 cm^{-1} for **2**, together with a relatively weak band near 1250 cm^{-1}, suggests that even in the solid state the mixed valence isomer has significant contribution. This is clearly in contrast to that expected from the structural point of view which is in complete agreement with the Mn^{III}−Cat assignment. The appearance of infrared bands characteristic of mixed valence semiquinone-catecholate complexes suggests that the $Mn^{III}(Cat)_2^-$ moiety is admixed with its mixed valence semiquinone-catecholate isomer, $Mn^{II}(SQ)(Cat)^-$.

Electrochemical Properties. Owing to the redox-active nature of the dioxolene ligands, ligand-based electrochemical activities are expected in both the complexes. The cyclic voltammetry was studied in acetonitrile for both the complexes, and the results are illustrated in Figure 4. In the available range of potentials, both **1** and **2** exhibit electrochemically quasireversible one-electron oxidation at +0.64 V ($E_{1/2}$ = 0.49 V, ΔE_p = 300 mV) and +0.66 V ($E_{1/2}$ = 0.54 V, ΔE_p = 240 mV) versus Fc/Fc^+, respectively. It is usually found in a family of metal−polyoxolene complexes that if different metal ions have the same oxidation states, the ligand-centered redox processes are characterized by similar free energy values.[16b] Therefore, these comparable redox couples are assigned to the oxidation of the Cat to

Table 4. UV−Vis−NIR Spectral Data of Complexes **1** and **2** at 25 °C

complex	solvent[a]	λ_{max}/nm (ϵ/dm^3 mol^{-1} cm^{-1})
1	MeCN	550 (5200), 360 (sh) (3850), 300 (11200), 1932 (140)
	DMF	570 (5120), 360(sh) (3810), 300(11230), 1932(145)
	MeOH	590 (5100), 360(sh) (3800), 300 (11400), 1930 (140)
	solid	540, 300, 1925
2	DMF	605 (672), 390 (2620), 284 (34640), 1927 (260)
	MeCN	600 (680), 348 (3592), 294 (9795), 250 (18368), 1930 (255)
	MeOH	710, 410(sh), 270
	solid	590, 360, 1920

[a] Solid state also indicated.

give a cationic di-semiquinone complex for **1** and a neutral mixed valence semiquinone-catecholate Mn^{III} complex for **2** as shown in eqs 6 and 7, respectively.

$$[Fe^{III}(bispicen)(Cl_4SQ)(Cl_4Cat)] \rightleftharpoons [Fe^{III}(bispicen)(Cl_4SQ)_2]^+ \quad (6)$$

$$[Mn^{III}(Cl_4Cat)_2]^- \rightleftharpoons [Mn^{III}(Cl_4Cat)(Cl_4SQ)] \quad (7)$$

This is substantiated by the observations made for the mixed valence $[Cr^{III}(Cl_4Cat)(Cl_4SQ)(L)]$ complexes.[14−16] The $E_{1/2}$ values observed for the Cat/SQ couple are similar to that observed for $[Cr^{III}(Cl_4Cat)(Cl_4SQ)(L)]$ complexes.[14−16]

Another irreversible oxidation wave at +0.96 V was also found for **1** (not shown in the figure) but not for **2**. This could be attributed to the oxidation of SQ to BQ resulting in the formation of $[Fe^{III}(bispicen)(Cl_4SQ)(Cl_4BQ)]^{2+}$ as shown in eq 8.

$$[Fe^{III}(bispicen)(Cl_4SQ)_2]^+ \rightleftharpoons [Fe^{III}(bispicen)(Cl_4SQ)(Cl_4BQ)]^{2+} \quad (8)$$

The irreversible electrochemical process might be due to the low coordination ability of the neutral *o*-benzoquinone ligand.[16]

In addition to the ligand-centered redox activity, an electrochemically quasireversible reduction wave is observed for **1** at −0.72 V ($E_{1/2}$ = −0.62 V, ΔE_p = 0.20 V) and an irreversible reduction wave at −0.55 V for **2**. In the case of **1**, it can be assigned as the reduction of the Fe^{III} to Fe^{II}. This value is, however, much higher than that observed for the anionic $[Fe(bpy)(Cl_4Cat)_2]^-$ complex[22a] but comparable to that observed for Fe^{III}/Fe^{II} reduction in $[Fe(L3)DBCat]^-$ complex[22b] where the process is irreversible. The electrochemical behavior observed for **1** is qualitatively similar to that observed for the $[Fe^{III}(bpy)(Cl_4SQ)(Cl_4Cat)]$ complex,[22a] but the potentials are shifted to more positive values in the present complex. The nature and reduction potential (−0.55 V) of **2** are similar to that observed for mononuclear manganese(III) complexes and attributable to the Mn^{III}/Mn^{II} redox couple.[22c]

UV−Vis−NIR Spectral Properties and VT Phenomenon. The electronic absorption spectra of both complexes were recorded in various solvents, and the relevant data appear in Table 4. Two intense bands in the 250−1100 nm region mainly characterize complex **1**. (i) In MeOH, it gives rise to an intense broad band which spans from 480 to 700

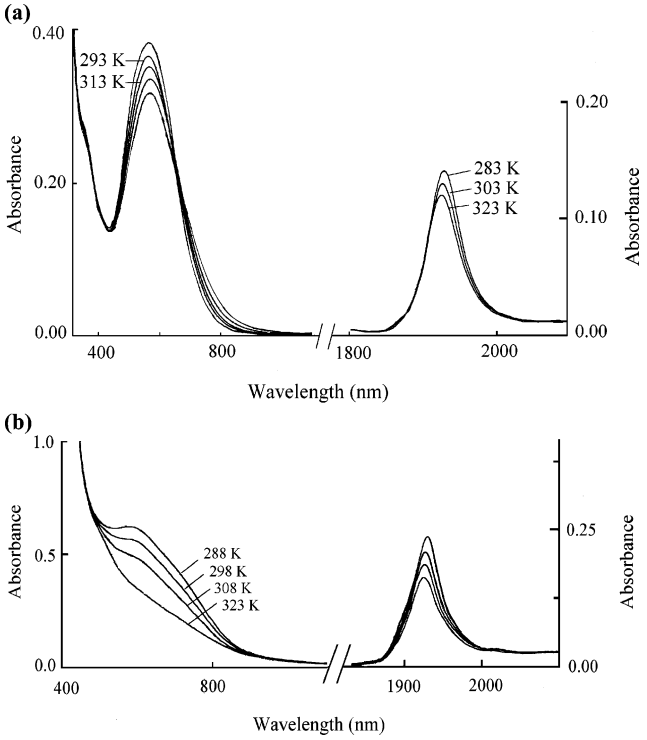

Figure 5. Temperature-dependent changes in the electronic absorption spectrum of complexes **1** and **2** showing reversible intramolecular one-electron transfer transition (VT) in DMF solution.

nm with $\lambda_{max} = 590$ nm and another more intense sharp band at $\lambda_{max} = 300$ nm. The lower energy band is assigned to the Cat $\rightarrow$ Fe^{III} CT transition whereas the higher energy bands are due to $\pi-\pi^*$ transition.[19] (ii) In MeCN and DMF, the lower energy bands were found to shift and appear at $\lambda_{max} = 550$ and 570 nm, respectively. The position of the higher energy band (300 nm), however, does not shift appreciably on changing solvents. The solvent dependence of the UV−vis spectrum of the mixed-valence semiquinone-catecholate iron(III) complexes, known as solvatochromic effect, was also previously observed.[13,19] Consistent with the structural and IR spectral features, the intervalence charge transfer band due to the semiquinone-catecholate transition was also observed at 1932 nm in MeCN and DMF which is somewhat higher-energy shifted compared to the previously reported mixed valence iron(III) complexes[25] and which could be attributed to the different substituents in the benzene ring of the catecholate moiety. (iii) The solid state electronic absorption spectrum taken in Nujol mull appears with noise, but the intervalence charge transfer band at 1925 nm is clearly observed.

Mixed valence semiquinone-catecholate iron(III) complexes so far characterized have failed to show any appreciable change in the electronic absorption spectra with change in temperature even though the thermodynamic conditions are favorable.[25] This is believed to be caused by the instability of the formed $Fe^{II}(SQ)_2$ species. We have recorded the electronic absorption spectrum of **1** in DMF at various temperatures as shown in Figure 5a. The increase in temperature is associated with a decrease of the 570 nm band with a clear isosbestic point at 650 nm. The same observation

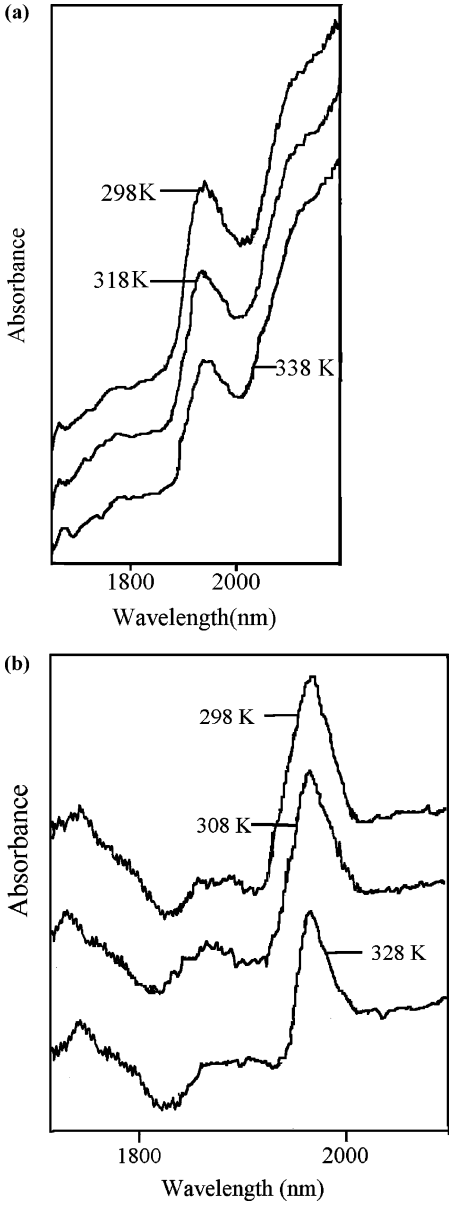

Figure 6. Temperature-dependent spectral changes in the 1900 nm region of complexes **1** (a) and **2** (b) showing intramolecular one-electron transfer transition (VT) in the solid state (Nujol mull).

was made in the 1932 nm region with an isosbestic point around 1880 nm. The appearance of isosbestic points is strong evidence for the existence of two equilibrating species in the solution.

The electronic absorption spectra in solid state in Nujol mull have also been recorded at different temperatures. Though these are noisy, the decrease of the 1925 nm bands with increase in temperature is clearly indicated (Figure 6a). The spectral changes amply support the valence tautomeric equilibrium as shown in eq 9.

$$[Fe^{III}(bispicen)(Cl_4Cat)(Cl_4SQ)] \rightleftharpoons [Fe^{II}(bispicen)(Cl_4SQ)_2] \quad (9)$$

To our knowledge, this is the first instance where an iron(III) complex is shown to exhibit valence tautomerism similar to Mn and Co *o*-dioxolene complexes.

The structural features associated with **2** essentially point to a mononuclear Mn^{III} complex, and the dinuclear nature is due to the extensive hydrogen bonding between the dicationic ligand and the coordinated oxygen atoms of the tetrachlorocatecholate ligands. It is, therefore, reasonable to consider that in solution complex **2** exists as a mononuclear Mn^{III} entity. Manganese complexes also show substantial solvatochromic effects. We recorded the electronic spectra of complex **2** in various solvents. The low solubility, however, restricted us to record the spectra in DMF, MeCN, and MeOH only. (i) A deep green solution is obtained when the crystals of **2** are dissolved in DMF and the spectrum is characterized by two transitions between 300 and 1100 nm. The low energy band spans over 540−860 nm with $\lambda_{max} =$ 605 nm, and another more intense sharp band appears at $\lambda_{max} =$ 390 nm. The intense higher energy bands are usually assigned to the $\pi-\pi^*$ transition. (ii) In acetonitrile, the electronic spectrum of **2** is qualitatively similar to that observed in DMF solution. The lower energy band does not shift appreciably and appears as a broad peak in the range 530−830 nm with $\lambda_{max} = 600$ nm. Three more bands in the region 200−400 nm are also observed in this instance, having $\lambda_{max} =$ 348, 294, and 250 nm. The electronic absorption spectra in DMF and acetonitrile are comparable to the mononuclear tetrabromocatecholate and/or tetrachlorocatecholate chelated manganese(III) complexes reported previously.[12] (iii) In methanol, complex **2** is sparingly soluble yielding a reddish brown solution which exhibits a weak broad band in the range 650−950 nm with $\lambda_{max} = 710$ nm and a single broad transition with $\lambda_{max} = 270$ nm. (iv) The solid state spectrum of the complex taken in Nujol mull is also similar to that observed in solutions showing two intense bands in the ranges 550−800 and 300−450 nm. A very striking feature of the spectra recorded either in solution or in the solid state is the appearance of a band centered at ca. 1927 nm both in solution and in the solid state. This is a characteristic intervalence charge transfer band typical for mixed charge semiquinone-catecholate transition metal complexes though the structural features are in agreement to a Mn^{III}−Cat formulation. The inference may be drawn to the existence of an equilibrium represented by eq 10 for each Mn^{III} unit. We suggest that the electronic absorption spectrum is dominated by the mixed charged species and the origin of the intervalence charge transfer band is associated with the mixed valence form, $Mn^{II}(Cl_4Cat)(Cl_4SQ)^-$.

$$Mn^{III}(Cl_4Cat)_2^- \rightleftharpoons Mn^{II}(Cl_4Cat)(Cl_4SQ)^- \qquad (10)$$

One of the notable features of the catecholate chelated manganese complexes is associated with their potential to show valence tautomerism in the solid as well as in solution. Changes in magnetism which are associated with the shifts in charge distribution have not been of use in the manganese series because the $Mn^{IV}(Cat)_2$, $Mn^{III}(SQ)(Cat)$, and $Mn^{II}(SQ)_2$ redox isomers all have an $S = {}^3/_2$ ground state. On the other hand, both $Mn^{III}(Cl_4Cat)_2^-$ and $Mn^{II}(Cl_4Cat)(Cl_4SQ)^-$ isomers have a ground state of $S = 2$. The changes in the electronic spectrum, however, are extensively used to observe the VT phenomenon for manganese complexes.

Figure 5b illustrates the electronic absorption spectral changes in the temperature range 10−50 °C for a DMF solution of **2**. It is observed that on increase in temperature the intensity of the lower energy LL′CT band at 1927 nm decreases appreciably with the corresponding decrease in intensity at 600 nm. This is concomitant with the change in color of the solution from deep green to light greenish yellow. Cooling of the greenish yellow solution, however, regenerates the deep green solution which suggests the reversibility of the phenomenon. Similar results have also been encountered during temperature dependent solid state spectral measurements where the complex is taken in Nujol mull (Figure 6b). Since the structural features are consistent with $Mn^{III}(Cat)_2^-$ formulation, the one-electron transfer from ligand to the metal should produce mixed valence semiquinone-catecholate species $Mn^{II}(SQ)(Cat)^-$, and consequently, an increase in the intervalence charge transfer band is expected. The observed decrease of the intensity of both 1927 nm and that of the visible region bands lies in the fact that the electronic absorption spectrum of **2** is dominated by the mixed valence species $Mn^{II}(SQ)(Cat)^-$ over its isomeric form $Mn^{III}(Cat)_2^-$. An increase in temperature of the solution results in an intramolecular electron transfer from Mn(II) to the oxidized SQ ligand shifting the equilibrium (10) toward the left, and thereby, a decrease in the intensity of absorption is observed at elevated temperatures. The small change in the electronic absorption spectra with temperature indicates that two opposing reactions are operative simultaneously, namely intramolecular electron transfer within the $Mn^{III}(Cat)_2^-$ unit to give $Mn^{II}(SQ)(Cat)^-$ which would tend to increase the intensity of the NIR band while intramolecular electron transfer within $Mn^{II}(SQ)(Cat)^-$ occurs to produce the $Mn^{III}(Cat)_2^-$ unit, decreasing the intensity of the absorbance.

Similar findings have also been made for the mixed valence 1D complex $[Mn^{III}_2(bispicen)(Cl_4Cat)_2(Cl_4SQ)_2]_n$, and $[Mn^{III}_2(bispictn)(Cl_4Cat)_2(Cl_4SQ)_2]_n$, which we have synthesized independently.[36b] Both of these complexes show an intervalence SQ-Cat transition near 1920 nm in DMF as well as in the solid state. The polynuclear $[Mn^{III}(\mu\text{-pyz})$-(3,6-DBSQ)(3,6-DBCat)$]_n$ and mononuclear $[Mn^{III}(4,4'\text{-bpy})$-(3,6-DBSQ)(3,6-DBCat)] complexes have been observed to undergo valence tautomerism in the solid state with a decrease in absorbance at 2090 and 2070 nm, respectively.[9,11]

EPR Properties of Complexes 1 and 2. Unlike the previously characterized mixed valence semiquinone-catecholato-iron(III) complexes,[13,19] complex **1** is EPR active. There is virtually no difference in the EPR spectra in the solid or in solution at 77 K. The spectrum of **1** in the solid state at room temperature is, however, quite different from that observed at 77 K. The spectra recorded under different conditions are illustrated in Figure 7a,b. The solid state spectrum of the complex at room temperature exhibits two broad transitions centered at $g = 1.92$ and 2.53 expected for the complexes having $S = 2$ ground state.[37a] The $S = 2$ state

(37) (a) Rancurel, C.; Lenzoff, D. B.; Sutter, J.-P.; Golhen, S.; Ouahab, L.; Kliava, J.; Kahn, O. *Inorg. Chem.* **1999**, *38*, 4753. (b) Harrop, T. C.; Tyler, L. A.; Olmstead, M. M.; Mascharak, P. K. *Eur. J. Inorg. Chem.* **2003**, 475.

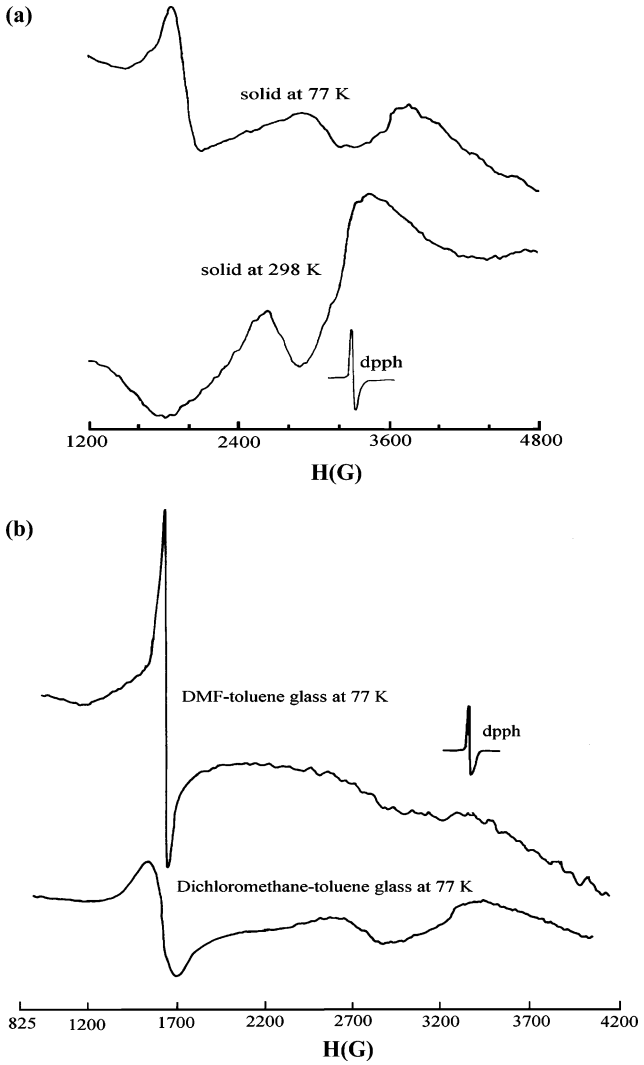

Figure 7. X-band EPR spectra of **1** (a) in the solid state at room temperature and at 77 K (spectrometer settings: field set at 3200 (G); scan range = 8000 G; frequency = 9.1 GHz; modulation amplitude = 1.25 × 10 G; power = 31 dB); (b) in DMF−toluene and DCM−toluene glass at 77 K (spectrometer settings: scan range = 5000 G; the rest are the same).

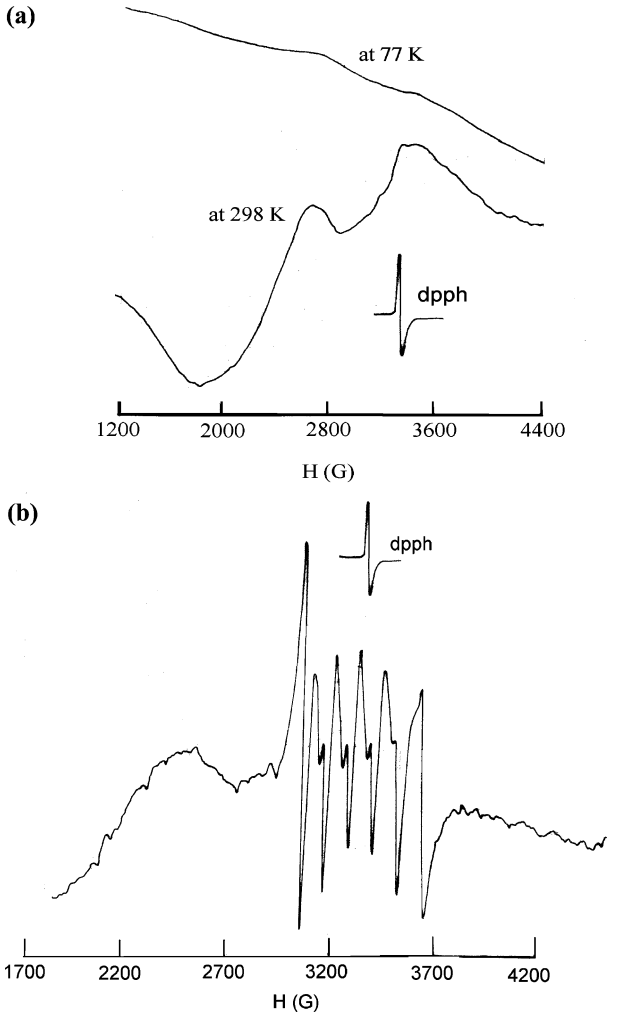

Figure 8. X-band EPR spectrum of **2** (a) in the solid state at room temperature and 77 K (spectrometer settings: scan range = 8000 G (at 77 K); 5000 G (at 298 K); frequency = 9.1 GHz; modulation amplitude = 1.25 × 10 G; power = 31 dB, gain = 3.2 × 10^3); (b) in DMF−toluene glass at 77 K (spectrometer settings: field set = 3200 G, the rest are the same).

for the present complex is due to the strong antiferromagnetic interaction between the Fe^{III} ($S = {}^5/_2$) ion and the semiquinone radical ($S = {}^1/_2$), and the temperature dependent magnetic susceptibility measurements (discussed below) confirm this. At 77 K, a strong signal at $g = 4.2$ typical for the high spin Fe^{III} complexes[37b] appears, and the intensity of the broad peaks observed at room temperature decreases appreciably. In DMF−toluene glass, only the strong signal in the $g = 4.2$ region expected for the pure $S = {}^5/_2$ state is observed. In CH_2Cl_2−toluene glass, the spectral pattern is quite similar to that observed in DMF−toluene glass; however, the weak signals corresponding to the $S = 2$ state in the $g = 2$ region could also be detected. The spectral pattern in CH_2Cl_2−toluene glass of **1** has a strong resemblance with the spectral features of $\{[Fe_2(pb)_4O(OOH)](ClO_4)\}^{2+}$ which has a ground spin state of $S = 2$ derived from the coupling of an $S = {}^5/_2$ and an $S = {}^1/_2$ ion in the diferric unit.[38] It is apparent that the local spin state of the central Fe^{III} ion changes with temperature and solvents. Halidobis(o-imino-benzosemiquinonato)-iron(III) complexes exhibit variable local spin state of the central Fe^{III} ion ranging from $S = {}^5/_2$ to pure $S = {}^3/_2$ which depends on the nature of the coordinated halide ligands.[39] The present observation also reminds us the temperature dependence of the EPR spectrum of the (3,5-di-*tert*-butylcatecholato)(3,5-di-*tert*-butylsemiquinone)(bipyridyl)cobalt(III) complex where VT has been established.[18] Previous experiments with mixed valence semiquinone-catecholate iron(III) complexes, however, did not show any intramolecular iron−quinone electron transfer as observed for manganese and cobalt complexes.

The solid state EPR spectrum of complex **2** at room temperature shows two broad transitions centered at $g = 1.99$ and $g = 2.8$ as in Figure 8. We suggest that the observed transitions arise from the mixed valence semiquinone-catecholate manganese(II) form, $Mn^{II}(Cat)(SQ)^-$, as the $Mn^{III}(Cat)_2^-$ isomer is expected to be X-band EPR silent.

(38) Hummel, H.; Mekmouche, Y.; Duboc-Toia, C.; Ho, R. Y. N.; Que, L., Jr.; Schünemann, V.; Thomas, F.; Trautwein, A. X.; Lebrun, C.; Fontecave, M.; Ménage, S. *Angew. Chem., Int. Ed.* **2002**, *41*, 617.
(39) Chun, H.; Weyhermuller, T.; Bill, E.; Weighardt, K. *Angew. Chem., Int. Ed.* **2001**, *40*, 2489.

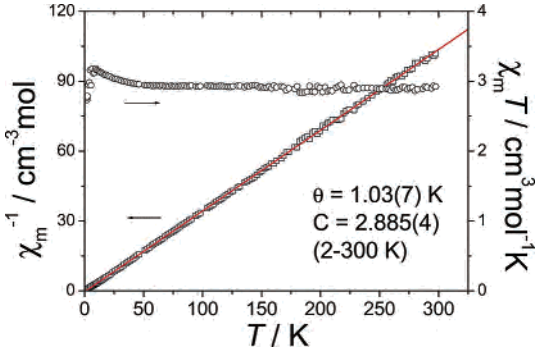

Figure 9. Temperature dependence of magnetic susceptibility of **1** measured in 10 kOe field. The solid line presents the best fit using the Curie−Weiss law.

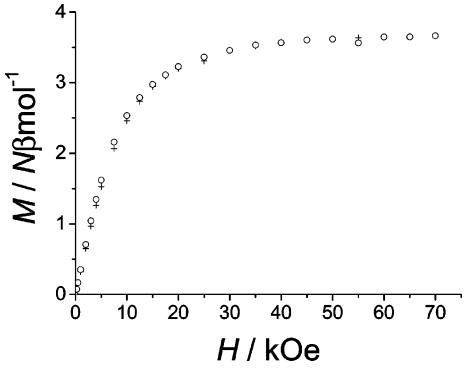

Figure 10. Field dependence of magnetization for **1** at 1.8 K.

Indeed, the [(*o*-nitronyl nitroxide-phenyl)diphenylphosphine oxide]bis(hexafluoroacetylacetonato)manganese(II), in which a radical is antiferromagnetically coupled with a Mn(II) center, exhibits similar EPR spectral features at room temperature.[37a] This strongly supports the existence of a $Mn^{II}(Cat)(SQ)^{-}$ isomer as inferred from infrared and electronic absorption spectral features. In DMF−toluene glass, the $g = 2.00$ region band is clearly resolved, and the spectrum shows a six-line hyperfine pattern (^{55}Mn, $I = {}^5/_2$) with $g_{||}$ value of about 2 ($A_{av} = 98$ G) and a weak signal at $g_{\perp} = 2.8$. The solid state spectrum at 77 K shows that both the broad bands observed at room temperature weaken in intensity. This is probably due to the fact that a decrease in the temperature increases the antiferromagnetic coupling between two semiquinone radical ions as complex **2** is dimeric in the solid state. There is no report of a frozen solution spectrum of these kind of species, but the powder EPR spectrum of Mn(salen)(3,5-DBSQ) displaying a broad isotropic signal at room temperature and liquid nitrogen temperature has been reported.[40]

Magnetic Properties of Complex 1. The magnetic measurements were done in the range 2−300 K for **1**. At room temperature, the $\chi_m T$ value is ca. 2.9 $cm^3\ mol^{-1}$ K, very close to the value 3.00 $cm^3\ mol^{-1}$ K for a spin state $S = 2$ and $g = 2.0$. As the temperature decreases, the $\chi_m T$ value remains almost constant down to ca. 50 K, and then shows a slight increase. The magnetic susceptibility in the whole temperature range (2.0−300 K) obeys the Curie−Weiss law ($\chi_m = C/(T - \theta)$) with $C = 2.885(4)$ $cm^3\ mol^{-1}$ K and $\theta = +1.03(3)$ K, Figure 9. The Curie constant C corresponds to a spin state $S = 2$ and $g = 2.0$. The field dependence of magnetization at 1.8 K shows a magnetization value of 3.67 $N\beta$ at 70 kOe which is close to the saturation value for the spin state, Figure 10. Therefore, the Fe^{III} complex can be viewed as an Fe^{III}−radical dimer, in which a very strong antiferromagnetic interaction between Fe^{III} and the radical results in an $S = 2$ spin state for the dimer which is consistent with the earlier observations with mixed valence semiquinone-catecholate high spin Fe^{III} complexes.[13,19] The slight increase of $\chi_m T$ upon cooling at low temperature and the small positive Weiss constant indicate a possibly very weak intermolecular ferromagnetic coupling between Fe^{III}−radical dimers. It should be mentioned here that because the valence tautomerism (VT) does not lead to the change of the total spin value of **1** and **2**, there will be no significant sign of the VT in the temperature dependent magnetic susceptibility data except abrupt change (high spin to low spin or vice versa) of the electronic configuration of the metal center after intramolecular electron transfer reactions.

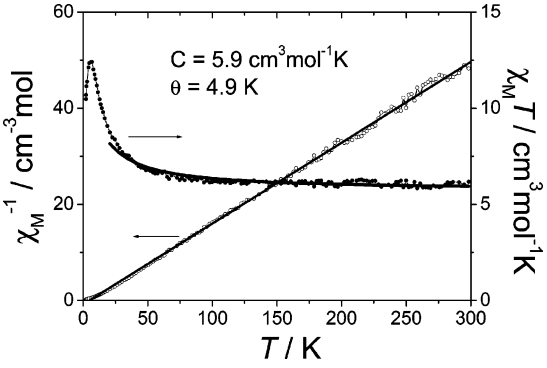

Figure 11. Temperature dependence of magnetic susceptibility of **2** measured in 5 kOe field. The solid line of χ_M^{-1} presents the best fit using the Curie−Weiss law, and the solid line of $\chi_M T$ presents the best fit using the theory model for ferromagnetically coupled Mn_2^{III}.

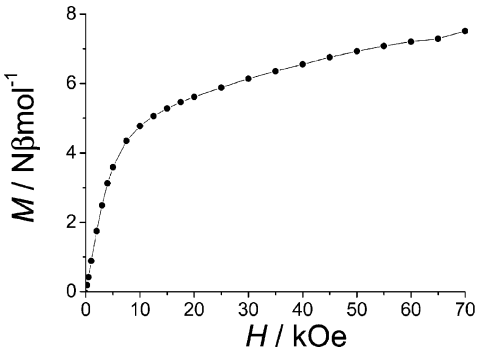

Figure 12. Field dependence of magnetization for **1** at 1.8 K.

Magnetic Properties of Complex 2. The temperature dependent magnetic susceptibility measurement for **2** was carried out in the temperature range 2−300 K at the external field of 5 kOe. The result is presented in Figure 11. At room temperature, the $\chi_m T$ value is ca. 6.0 $cm^3\ mol^{-1}$ K which fits well with the value of 6.0 $cm^3\ mol^{-1}$ K for two spin-only uncoupled Mn^{III} ions and consistent with the solid state structural characterization. As the temperature decreases, the $\chi_m T$ value increases slightly in the high temperature range

(40) Kessel, S. L.; Emberson, R. M.; Debrunner, P. G.; Hendrickson, D. N. *Inorg. Chem.* **1980**, *19*, 1170.

and increases rapidly to a maximum of 12.4 $cm^3\ mol^{-1}$ K at ca. 6.9 K, and then, it drops to 10.5 $cm^3\ mol^{-1}$ K at 2.2 K. The best fitting of the data from 2 to 300 K with the Curie−Weiss law gives the Curie constant $C = 5.9\ cm^3\ mol^{-1}$ K and the Weiss constant $\theta = +5.9$ K. The field dependence of magnetization at 1.8 K shows a magnetization value of 7.52 $N\beta$ at 70 kOe, which is close to the saturation value for two Mn^{III} ($S = 2$) ions (Figure 12). The shape of the plot of $\chi_m T(T)$ and the overall positive Weiss constant may indicate the existence of ferromagnetic coupling between the two neighboring Mn^{III} (MnA and MnB in the dimeric unit, see Figure 3) ions bridged by μ_2-oxygen atoms. This observation is similar to that reported previously in which the dimeric Mn^{III} is formed via a weak bonding involving μ_2-oxygen.[41] By considering the exchange interaction Hamiltonian $\mathbf{H} = -2JS_1 \cdot S_2$, we get the coupling constant $J = 2.0$ (1) cm^{-1} and $g = 1.95$ (1) using the data from 20 to 300 K. The best fit of $\chi_m T(T)$ can be seen in Figure 9. The present J and g values are consistent with those of Mn^{III} dimer bridged by two oxygen atoms reported elsewhere.[41]

Acknowledgment. S. Goswami and A. Panja would like to thank the Council of Scientific and Industrial Research, New Delhi, for financial support, and P. Banerjee is also thankful for a grant for a project.

Supporting Information Available: Crystallographic data in CIF format. This material is available free of charge via the Internet at http://pubs.acs.org.

IC049579I

(41) Miyasaka, H.; Clérac, R.; Ishii, T.; Chang, H.-C.; Kitagawa, S.; Yamashita, M. *J. Chem. Soc., Dalton Trans.* **2002**, 1528.